Shear stress controls prokaryotic and eukaryotic biofilm communities together with EPS and metabolomic expression in a semi-controlled coastal environment in the NW Mediterranean Sea

Aurélie Portas, Nathan Carriot, Raphaëlle Barry-Martinet, Annick Ortalo-Magné, Houssam Hajjoul, Bruno Dormoy, Gérald Culioli, Nolwenn Quillien, Jean-François. Briand

Environmental Microbiome

RESEARCH

Open Access

Shear stress controls prokaryotic and eukaryotic biofilm communities together with EPS and metabolomic expression in a semi-controlled coastal environment in the NW Mediterranean Sea

Aurélie Portas[1,2*], Nathan Carriot[2], Raphaëlle Barry-Martinet[2], Annick Ortalo-Magné[2], Houssam Hajjoul[3], Bruno Dormoy[4], Gérald Culioli[2,5], Nolwenn Quillien[1] and Jean-François. Briand[2]

Abstract

While waves, swells and currents are important drivers of the ocean, their specific influence on the biocolonization of marine surfaces has been little studied. The aim of this study was to determine how hydrodynamics influence the dynamics of microbial communities, metabolic production, macrofoulers and the associated vagile fauna. Using a field device simulating a shear stress gradient, a multi-scale characterization of attached communities (metabarcoding, LC–MS, biochemical tests, microscopy) was carried out for one month each season in Toulon Bay (northwestern Mediterranean). Shear stress appeared to be the primary factor influencing biomass, EPS production and community structure and composition. Especially, the transition from static to dynamic conditions, characterized by varying shear stress intensities, had a more pronounced effect on prokaryotic and eukaryotic beta-diversity than changes in shear stress intensity or seasonal physico-chemical parameters. In static samples, mobile microbe feeders such as arthropods and nematodes were predominant, whereas shear stress favored the colonization of sessile organisms and heterotrophic protists using the protective structure of biofilms for growth. The increase in shear stress resulted in a decrease in biomass but an overproduction of EPS, specifically exopolysaccharides, suggesting an adaptive response to withstand shear forces. Metabolite analysis highlighted the influence of shear stress on community dynamics. Specific metabolites associated with static conditions correlated positively with certain bacterial and algal groups, indirectly indicating reduced grazer control with increasing shear stress.

Keywords Shear stress, Marine biofilms, Biofouling, Multi-omics, EPS analysis, Metabarcoding, Metabolomics, Microscopy

*Correspondence:
Aurélie Portas
aurelie.portas@hotmail.com
Full list of author information is available at the end of the article

Introduction

Biofilms are multitrophic communities, with a high phylogenetic diversity (prokaryotes and eukaryotes), embedded in a matrix of self-produced extracellular polymeric substances (EPS) [1]. Such a complex microbial cosmos ultimately determines biofilms functionality [2]. In marine environments, this life strategy provides better protection and chance of survival in the face of environmental stress allowing rare planktonic organisms to thrive and become abundant [3]. Biofilm development is influenced by various chemical, biological, and physical factors, including nutrients, salinity, predation, temperature, depth, substrate, and hydrodynamic forces generated by seawater movement around the colonized surfaces [4].

Previous research on measurement of shear stresses in marine sediments and river environments has expanded over time, with the development of a variety of laboratory and in situ devices and methods [5–7]. However, many studies on hydrodynamic forces have focused on the effects of shear stress on bacterial biofilms formed with cultures of pathogenic strains, numerical models or in freshwater ecosystems under controlled conditions [8, 9]. Based on laboratory experiments, it has been shown that flow intensity can influence biofilm properties such as community composition, physical structures, and growth [10–12]. Under low shear forces, biofilms are less dense, more porous, and thicker. This type of architecture promotes nutrient transport within the biofilm, which increases its activity, and thus its thickness [13, 14]. Conversely, higher shear rates result in more compact and dense biofilms, with a less heterogeneous morphology [10, 11]. Monospecific biofilms can change their metabolism in response to an increased shear stress: the production of exopolymers, mainly polysaccharides, becomes higher, providing a more rigid structure through a greater cohesion between microbial cells [15]. Moreover, very high shear forces (> 3 Pa) can lead to deformation of biofilms and even to their subsequent detachment from the colonized surfaces [16]. However, these examples were mainly conducted on biofilms composed of a single strain, whereas marine biofilms are typically highly diversified.

In marine ecosystems, current velocities and the resulting hydrodynamic forces are composed of chaotic motions, which can be defined in two loading categories: normal forces are represented by pressure fields, as waves acting on offshore systems, while tangential forces induce shear stress, typical of hydrodynamics of tides or moving ships. This understanding of hydrodynamic forces is of crucial importance for the control of biological colonization on marine artificial substrates, including marine renewable energy (MRE) systems, underwater sensors and ship hulls or microplastics [17–19]. To date, only a few studies have investigated such physical factors on marine biofouling diversity and functions [20–22].

In this study, shear stress, a hydrodynamic component, was isolated to explore variations in microbial community dynamics, biofilm metabolic production and interactions with macrofouling and associated fauna. These differences were examined in static and dynamic samples with different shear stress intensities. We also investigated whether stress-induced changes alter the EPS matrix of biofilms. Our hypothesis was that the effect of shear stress would be a major stress for biofilm diversity and functions, perhaps more structuring than physicochemical parameters of the seawater over the four seasons studied. We thus predicted a shift in community composition, with hydrodynamic stress-adapted taxa and EPS. To evaluate our hypothesis, taxonomic diversity, EPS and metabolic production of marine biofilms were analyzed in response to a gradient of shear stress intensity across seasons in a northwestern Mediterranean bay.

Materials and methods

Experimental design

The field experiment was conducted in Toulon Bay (French Mediterranean Sea; 43°06′25″N; 5°55′41″E) at the four seasons for one month from August 2020 to May 2021. Immersions were performed on sandblasted polyvinyl chloride (PVC) panels. Sampling design included static and dynamic immersions (Supplementary 1 and Figure S1) submerged to a depth of −1 m below the surface. For dynamic immersions, 18 panels (25 cm × 5 cm) were set from the center to the edge of a rotation drum which was directly immersed in seawater. The drum rotated at a speed of 2.7 $m.s^{-1}$, simulating shear velocities ranging from 0 to 2.7 m s^{-1}, similar to the range of natural conditions in the Mediterranean Sea [23, 24]. A gradient of four speeds, from S_1 to S_4, was set (S_1 = 0.31 m s^{-1}; S_2 = 0.98 m s^{-1}; S_3 = 1.58 m s^{-1} and S_4 = 2.26 m s^{-1}). For static immersions (S_0 = 0 $m.s^{-1}$), PVC panels (4 panels 21 × 29.7 cm and 4 panels 5 × 5 cm) were used. Panels were immersed in the same area as the rotor, but far enough away that the induced currents did not affect their colonization. It is assumed that these conditions will remain static, even though they are also subjected to internal water movements within Toulon Bay.

Confocal laser scanning microscopy (CLSM) and low vacuum scanning electron microscopy (LV-SEM)

Biofilm 3D structures were observed with a CLSM (Zeiss Confocal LSM 510 Meta; Göttingen, Germany). A multi-labeling study was performed with three fluorophores, SYTO 61, concanavalin A and FITC (fluorescein isothiocyanate), which were used for labelling DNA,

polysaccharides, and proteins, respectively (see Supplementary 2 for more details). Images were acquired with a×63 oil-immersion objective and analyzed for simultaneous visualization of EPS matrix and microbial cells. Biofilms formed in situ were also directly observed by LV-SEM (JSM-6510 Series Scanning Electron Microscope; Musashino, Japan, field emission gun: 20 kV in a vacuum of 30–100 Pa).

Molecular analyses and bioinformatic process

Biofilms were collected from three replicate panels, with three panels for S_0 (5×5 cm) and three panels from S_1 to S_4 (25 cm×5 cm). The biofilms were scraped with a sterile scalpel and stored in a 50 ml tube at -20 °C until DNA extraction. Before scraping, each panel was individually rinsed with sterile seawater to remove any loose or poorly attached organisms, so that only firmly attached biofouling was collected. DNA extraction was performed with the Qiagen DNA Power Biofilm kit following the manufacturer's instructions. 16S rRNA [25], 18S rRNA [26] and the mitochondrial cytochrome oxidase I (COI) [27] genes were amplified for all the samples together with negative controls (see Supplementary 3 for methods). Samples ($n=180$, 60 per each primer pair) were sequenced using Illumina MiSeq platform (2×300 bp). All data are available from the NCBI BioProject database (accession number PRJNA1052431).

The bioinformatics workflow for paired-end data included Cutadapt (v. 3.1) for adapter trimming, DADA2 (v. 1.20) for amplicon sequence variant (ASV) inference, and FROGS (v. 4.0.1) for ASV assignment. Taxonomic assignment using SILVA (v. 138.2) database for 16S rRNA, PR2 (v. 4.14.0) for 18S rRNA and BOLD (v. 2023) for COI. For further details regarding the taxonomic affiliation and statistical analyses conducted within R environment, see Supplementary 3 and 4.

Untargeted LC–MS-based metabolomics analysis

The metabolomics workflow used for this study was previously described in Portas et al. [28]. A detailed description of sampling, samples processing, liquid chromatography-mass spectrometry (LC–MS) analysis, data extraction, data analyses and metabolome annotation can be found in Supplementary 5. Briefly, raw data were converted into ".netCDF" files using DataAnalysis (version 4.3; Bruker Daltonics, Germany) and processed with MZmine-2.58 [29]. The first step was the construction of the final data matrix, with parameters listed in Table S1. The data were then filtered according to Carriot et al. [30], accounting for the signal-to-noise ratio, coefficient of variation, and correlation coefficient. The resulting data matrix was normalized (sum of the peak intensities), $\log_{10}$-transformed, mean-centered and statistically analyzed using the Metaboanalyst 5.0 online platform [31].

Extraction and biochemical composition of EPS

EPS were extracted from biofilms and transferred to a 50 mL sterile Falcon tube containing 10 mL of Artificial Sea Water (ASW). Three fractions were recovered through successive centrifugation and precipitation steps: the colloidal fraction (CF), the loosely bound fraction (LBF), which could potentially include intracellular polymers due to a partial cell lysis caused by sonication), and the residual fraction (RF) composed of intact cells and cell residues. The EPS fractions (CF and LBF) of each sample were lyophilised, weighed and subjected to biochemical composition analysis using colorimetric methods (see Supplementary 6 for more details). The total biomass was determined as the sum of the three fraction weights.

Multi-omics analysis

Metabarcoding and metabolomics datasets were combined using DIABLO in the R package mixOmics [32]. The three metabarcoding sets of raw data were filtered to retain only ASVs representing more than 1% of sequences and were normalized using the CLR transformation. We selected an optimal set of variables (25 metabolites, 44 16S rRNA ASVs, 24 18S rRNA ASVs, and 13 COI ASVs) that played a significant role in discriminating samples on the basis of their immersion mode (static *vs.* dynamic) using the "tune.block.splsda" function. A correlation network was then constructed, showing only positive strong correlations (with a threshold of $r \geq 0.75$) among the selected variables. This network was imported and analyzed using Cytoscape (v. 3.9).

Results

Seawater characteristics

The temperature ranged from 11.4 °C in winter to 21.6 °C in summer. Salinity and pH remained constant at around 38 and 8, respectively (Table S2). Dissolved oxygen concentrations ranged from 86 to 96% saturation, with lower values observed in winter than in summer and spring. Nitrogen concentrations, including nitrates and nitrites, were high in spring, while phosphate concentrations were high in winter. DOC values varied considerably, particularly in autumn (133.95 ± 77.40) and spring (174.69 ± 116.26).

Effects of shear stress on biomass and microscopic visualization

Compared with autumn and winter, biomass was higher in summer (Wilcox test, $p<0.05$) (Fig. 1A). Regardless of the season, biomass followed a two-step response,

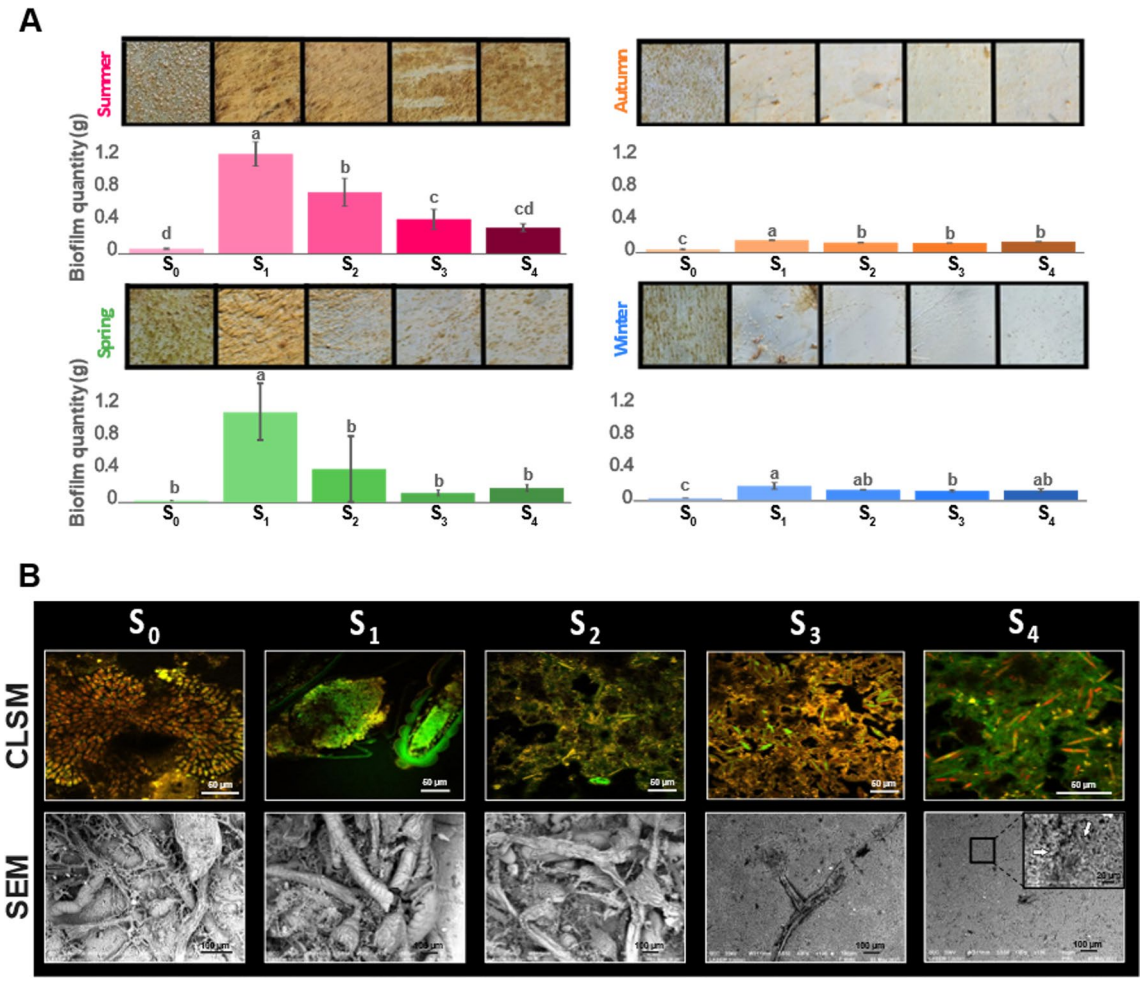

Fig. 1 Biomass with macroscopic, CLSM and SEM pictures of biofilms formed on the surface of 5 × 5 cm panels immersed for 30 days in the NW Mediterranean Sea under a shear stress gradient: $S_0 = 0$ m.s^{-1}; $S_1 = 0.31$ m.s^{-1}; $S_2 = 0.98$ m.s^{-1}; $S_3 = 1.58$ m.s^{-1} and $S_4 = 2.26$ m.s^{-1}. **A** Biofilm biomass (dry weight) with pictures of biological colonization according to shear stress intensities and seasons of immersion. Letters above barplots represent pairwise comparisons between each shear stress conditions according to the season. **B** Top pictures: observation by CLSM of biofilms in spring. Proteins appear in green (FITC), polysaccharides in orange (Concanavalin A) and DNA in red (SYTO61). Autofluorescence of chlorophyll appeared in red. Bottom pictures: SEM observations of biofilms in spring. White arrows indicate diatoms embedded in the EPS matrix

showing significantly higher values in S_1 compared to S_0 (static mode), but with decreasing biomasses from S_1 to S_4 except in winter, S_4 values approaching those obtained in S_0. Biofouling that developed in spring under low shear stress conditions (S_0 to S_2) showed different sizes and shapes of micro- and macroorganisms, as shown by SEM images (Fig. 1B).

In contrast, biofilms obtained in highly dynamic conditions (S_3 and S_4) appeared flatter and consisted mainly of bacteria and diatoms embedded in an EPS matrix. CLSM showed that in S_0, Syto61-stained cells (red) formed spherical structures while FITC-staining (green) highlighted cell walls and protein components. Conversely, S_3 and S_4 showed biofilms as thin layers with numerous diatoms (chlorophyll in chloroplasts and raphe stained red and green, respectively) embedded in an EPS matrix composed mainly of polysaccharides and proteins (orange and green, respectively).

Diversity and composition of the prokaryotic and eukaryotic communities across different shear stress intensities

Prokaryotic diversity was slightly affected by shear stress variations across seasons (Fig. S2). Significant differences were only observed between S_0 and S_4 richness in winter and spring. The Shannon index displayed also significant differences between S_0 and S_4 except in summer (Figs. S3, S4). Eukaryotic richness

(Fig. S2) showed less clear trends. The Chao 1 index values for 18S rRNA showed significant differences only in autumn, indicating an increase in diversity between the S_0 and S_1 conditions. COI diversity indices showed a decrease between S_0 and low dynamics (S_1/S_2), followed by an increase in S_4 in summer and winter. In autumn, richness increased between S_0 and dynamic conditions (S_1 to S_4), while in spring it decreased.

Furthermore, similar clustering patterns could be observed for all three markers. Seasons and shear stress intensities showed a significant influence on communities, as indicated by NMDS (PERMANOVA, $p < 0.0001$) (Fig. 2). In addition, pairwise comparisons revealed significant.

differences between communities in S_0 compared to all dynamic conditions (S_1–S_4) ($p < 0.05$). The distance values indicated that the change in immersion mode shaped communities more than the different shear intensities (Fig. S5, Table S4). Envfit analysis identified temperature, nitrite, nitrate, and pH as the main variables associated with NMDS ordination for 16S and 18S rRNA data, while salinity, silicate, nitrite and nitrate were associated with COI data (Table S3). Shear stress had a significantly higher impact on prokaryotic communities than variations in environmental parameters. This is suggested by the higher distance observed between S_0 and S_4 at all seasons. Conversely, the impact on eukaryotic communities appeared similar (Table S4).

Prokaryote community was dominated by *Rhodobacteraceae*, *Flavobacteriaceae*, *Pseudoalteromonadaceae* and *Vibrionaceae* (Fig. 3). *Flavobacteriaceae* and *Saprospiraceae* dominated in summer/autumn, whereas *Rhodobacteraceae* dominated in winter/spring. *Winograskella* was the main genus in static conditions in all seasons, while *Tenacibaculum* and *Aquibacter* were dominant in dynamic samples, with a decrease in autumn. Notably, *Sulfurovum* and *Mycoplama* increased in shear stress samples in autumn/winter. Similar trends were observed for the genus *Anaerolinea* in summer, and genera of Gammaproteobacteria (*Pseudoalteromonas* and *Vibrio*) in spring. Among *Roseobacteraceae*, *Roseovarius*, *Sulfitobacter* and *Litoreibacter* were predominant genera in dynamic samples, especially in winter and spring.

The eukaryotic community, which combined 18S rRNA and COI data, showed seasonal patterns. For instance, Dinophyceae were only present in spring in dynamic samples (Fig. 3). Hydrozoan communities also showed seasonal variations: *Bougainvillia* dominated in autumn/winter in dynamic samples, while *Obelia* dominated in spring/summer, decreasing as shear stress increased, with the appearance of *Hydractinia* and *Coryne*. Arthropods (Copepoda and Malacostraca), the nematode *Chromadorina*, the rhodophyte *Ceranium* (Florideophycideae), and the mollusc *Eubranchus* were found on the static panels. Diatoms and some members

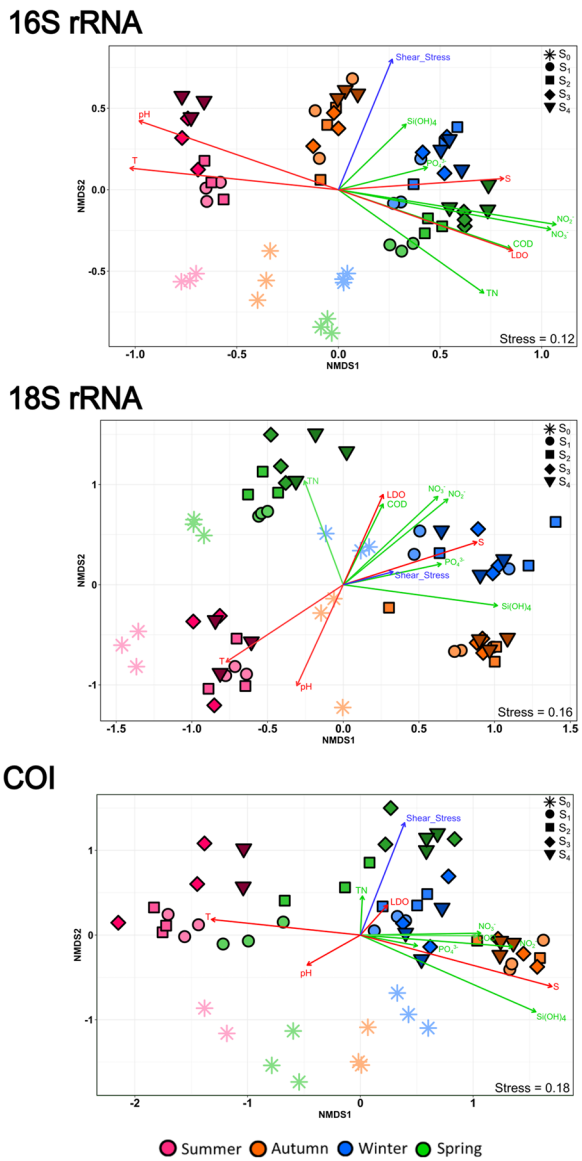

Fig. 2 NMDS showing biofouling community structure based on 16S rRNA (top), 18S rRNA (middle), and the COI (bottom) genes. The Bray–Curtis distance was used for 16S rRNA data whereas the Jaccard distance was used for 18S rRNA and COI data. The red vectors represent the physical variables (T: temperature; pH; LDO: Luminescence dissolved oxygen; S: salinity). The green vectors represent the chemical variables (TN: total nitrogen; DOC: dissolved organic carbon; NO_3^-: nitrate; NO_2^-: nitrite; PO_4^{3-}: phosphate; $Si(OH)_4$: silicate) and the blue vector represents the shear stress intensity (envit'function). Each point represents a sample, and the colors represent the seasons. For each shear stress the color is graded from the lightest for the lowest shear stress to the darkest for the highest shear stress

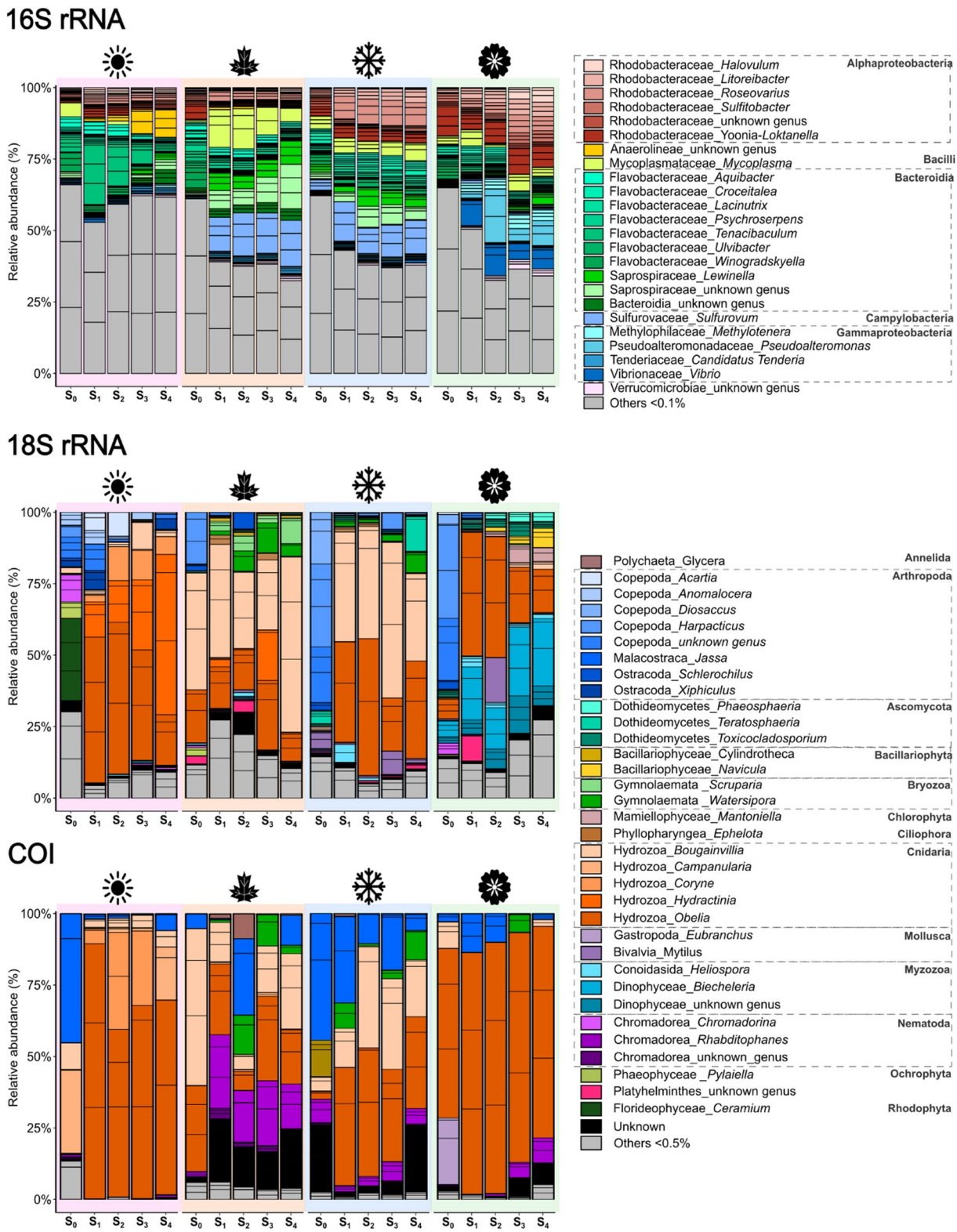

Fig. 3 Taxonomic composition of biofouling communities identified with 16S rRNA, 18S rRNA and COI genes according to shear stress and season. : Summer; : Autumn; : Winter; : Spring

of the Dothiomycetes (such as *Phaosphaeria* and *Toxicocladosporium*) were also dominant in spring dynamic samples.

Taxa specifically associated with shear stress conditions

Between 10 and 22% of the ASVs (representing 59–71% of the reads) were common and formed the prokaryotic and eukaryotic core communities (Table 1). The number of unique ASVs for both prokaryotic and eukaryotic communities was higher in static samples than for shear stress intensities taken individually. However, taken as a whole, there were more unique ASVs associated with dynamic conditions than with static ones.

Heat tree analyses revealed that genera significantly differed between static (S_0) and dynamic (S_1–S_4) conditions (Fig. 4). Some genera of *Rhodobacteriaceae*, in particular *Roseovarius* and *Litoreibacter*, showed a significantly higher relative abundance of ASV in samples exposed to shear stress. Among this group, the genus *Salinihabitans* was specific to these conditions.

and showed a marked increase in summer and spring (Fig. S6). Within the *Gammaproteobacteria* group, some genera such as *Pseudoalteromonas* and *Vibrio* were discriminant in dynamic samples regardless of season. In addition, the genus *Thiothrix* was also identified as discriminatory in dynamic conditions and specific to summer and autumn. In contrast, most genera of *Flavobacteriaceae* were discriminant under static conditions, particularly the genus *Ochrovirga*, which was relatively abundant regardless of season (Figs. 4, S6).

Regarding eukaryotic communities, hydrozoans, specifically the genus *Obelia*, and diatoms were found in significantly higher relative abundance in dynamic samples (Fig. 4). The ciliate genera *Hypocoma* and *Ephelota* dominated under dynamic conditions too. Furthermore, some genera of this group, including *Euplotes*, *Loxophyllum* and *Disteria*, were specific in dynamic samples during autumn and winter seasons. (Fig. S6). Bryozoans, mainly *Watersipora* and *Scuparia*, were also specific genera in dynamic samples over the same period. In contrast, static samples showed a significantly higher relative abundance of copepods, nematoda and red and brown algae. In winter and autumn, static samples also showed a dominance of Dinophyceae, including the genera *Amphidinium* and *Prorocentrum*, while in spring, the relative abundance of *Eubranchus* (Gastropoda) increased.

Variations of the metabolic expression depending on shear conditions

With regard to variations in metabolic expression in relation to the conditions of shear, PCA results showed that, regardless of season, samples were discriminated along the second axis of the PCA plot, mainly by immersion mode (static *vs*. dynamic) (Fig. S7). Using a supervised PLS-DA model (Fig. S8A), we identified chemomarkers for each immersion mode and performed discriminative

Table 1 Percentages of ASVs and sequences including all seasons for the 16S rRNA, 18S rRNA and COI genes. The core community corresponds to the shared ASVs. Specific ASVs correspond to unique ASVs for each shear stress intensity including the static condition. Specific dynamic includes ASVs only observed in dynamic samples taken together (S_1/S_2/S_3 and S_4)

	16S rRNA		18S rRNA		COI	
	ASVs	Reads	ASVs	Reads	ASVs	Reads
Core community	22 ± 3	59 ± 13	16 ± 3	71 ± 14	10 ± 6	60 ± 19
Specific static S_0	14 ± 1	4 ± 1	11 ± 2	4 ± 3	19 ± 9	7 ± 6
Specific dynamic (S_1, S_2, S_3 and S_4)	38 ± 5	27 ± 11	48 ± 12	15 ± 9	54 ± 13	26 ± 20
Specific S_1	3 ± 3	0.2 ± 0.2	5 ± 1	0.1 ± 0.1	4 ± 2	0.3 ± 0.4
Specific S_2	2 ± 1	0.1 ± 0.1	4 ± 2	0.2 ± 0.1	3 ± 1	0.5 ± 0.8
Specific S_3	2 ± 1	0.1 ± 0.02	4 ± 2	0.4 ± 0.6	5 ± 2	0.1 ± 0.1
Specific S_4	2 ± 1	0.2 ± 0.1	4 ± 2	0.5 ± 0.5	10 ± 6	0.7 ± 1.1

(See figure on next page.)

Fig. 4 Heat trees were constructed based on the dataset of the three markers (16S rRNA gene, 18S rRNA gene and COI) plotted at the genus level. Each connected node represents a different taxonomic level. All seasons were merged to observe the effect of immersion mode (i.e. static vs. dynamic) regardless of season. The size of the nodes is proportional to the relative abundance that makes up that taxonomic level. The nodes are coloured according to the log2 ratio of the average proportion of each rank as a function of immersion mode. The colour assigned to each taxon reflects the differential abundance between two immersion modes: red corresponds to taxa whose differential abundance is higher under static conditions and blue corresponds to taxa whose differential abundance is higher under dynamic conditions. The data were filtered to retain the 40 most abundant in both the static and dynamic conditions for each marker

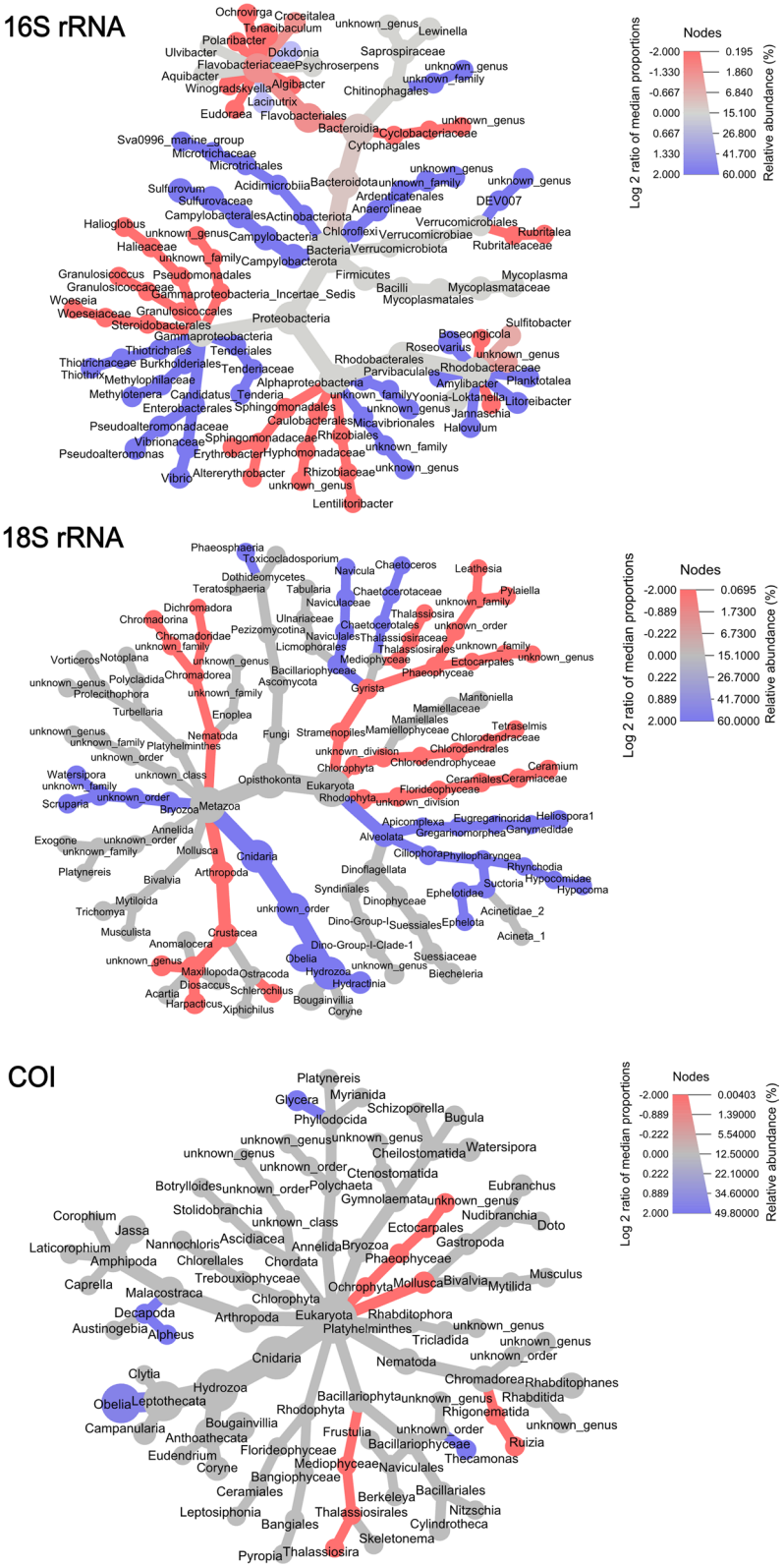

Fig. 4 (See legend on previous page.)

m/z feature annotation (VIP scores > 2.0) (Fig. S8B). Among the first 15 putatively annotated VIPs (Table S5), 14 compounds were discriminating in static samples, while dimethylsulphoniopropionate (DMSP) was the only chemomarker in dynamic conditions. Some families of molecules were identified on the molecular network especially in the static samples, most of them were *lyso*-DGTA and simple fatty acids (Fig. S9). Conversely, phosphatidylethanolamines, phosphatidylcholines and sphingosines were identified in dynamic samples.

Changes in EPS matrix in response to variations in shear stress intensity and season

Samples collected in winter and autumn under dynamic conditions were characterized by low amounts of biofilms. After EPS extractions, residual biofilm fractions obtained showed the highest variability, with significantly higher amounts in S1 compared to other conditions, especially in summer and spring (Fig. S10). Both colloidal and loosely bound EPS fractions showed significant weight differences between static and dynamic samples, with lower values in static conditions and similar values in dynamic conditions. Their proportions in the total biomass were higher with increasing shear stress intensities, especially in autumn and winter (Fig. S11). Polysaccharides dominated colloidal and loosely bound EPS fractions while only small amounts of proteins were observed. Proteins were present in sufficient amounts to be detected but their proportions were lower in summer and higher in spring compared to those observed for polysaccharides (Table S6). A PCA model (Fig. 5, Table S6) showed that polysaccharides and uronic acids were associated with static samples across all seasons on the PC1 axis (63.1% of total variance). Proteins, in both colloidal and loosely bound fractions, were correlated with low shear stress intensities, especially in summer and spring.

A multi-omics approach to identify key variables associated to shear stress

A multiblock PLS-DA model was constructed by combining four datasets (16S rRNA, 18S rRNA, COI and metabolomics) highlighting the most discriminating variables between static and dynamic conditions. The multi-omics network (Fig. 6) revealed two distinct clusters: the first cluster included ASVs (most of which were prokaryotes, such as the genera *Ochrovirga*, *Erythrobacter*,

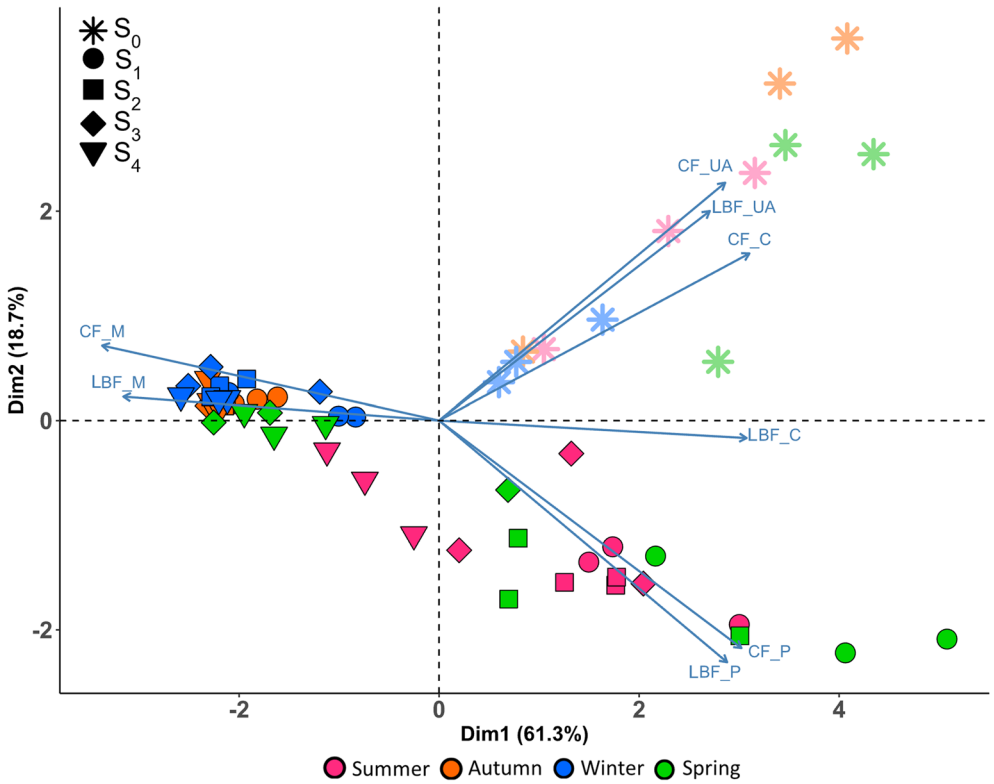

Fig. 5 Structure of EPS composition depending on season and shear stress intensity using a PCA biplot including the colloidal (CF) and the loosely bound fractions (LBF). Abbreviations mean: CF_C: Colloidal Fraction Carbohydrates, LBF_C: Loosely Bound Fraction Carbohydrates, CF_UA: Colloidal Fraction Uronic Acids, LBF_UA: Loosely Bound Fraction Uronic Acids, CF_P: Colloidal Fraction Proteins, LBF_P: Loosely Bound Fraction Proteins, CF_M: Colloidal Fraction Mass, LBF_M: Loosely Bound Fraction Mass. The colors represent the seasons

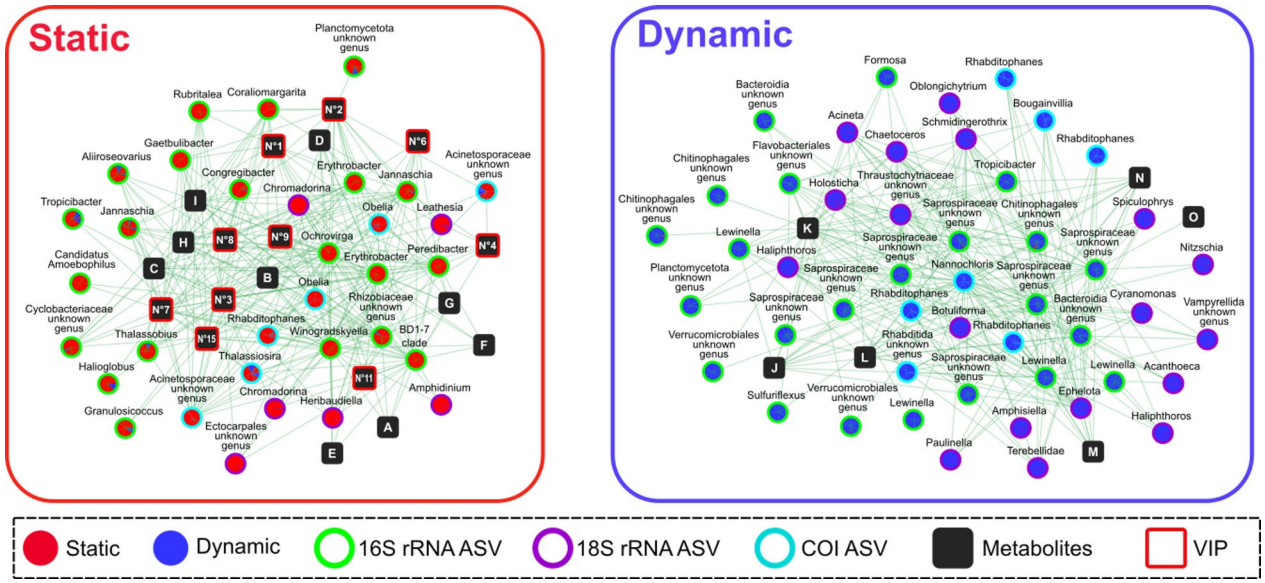

Fig. 6 Correlation network (PLS-DA multi-blocks) of the metabolome and biofilm communities. Discriminating ASVs (green circles for 16S rRNA; purple circles for 18S rRNA and blue circles for COI) and metabolites (black squares) are positively connected (green lines) with a threshold greater than 0.75. VIPs are indicated in the network with a red border and the letters correspond to the ID number indicated in Table S5. The pie-chart within each node revealed the distribution of each ASV across the different sample groups (red: static immersion mode, blue: dynamic immersion mode)

Winosgradskyella) and metabolites (VIPS like Pheophorbide a, nitenin and Stigmatellin Y) that were positively correlated and specifically present in static samples. Eukaryotes like *Chromadorina* (Nematoda), Amphidinium (Dinophyceae) and several Phaeophycean such as *Acinetosporaceae* and *Heribaudiella* appeared also as central actors of these communities. The second cluster was composed of numerous ASVs and 6 unidentified metabolites, which were all specific to dynamic samples. Several bacterial genera were positively correlated with microeukaryotes such as *Acineta* (Cilliophora), *Chaeotoceros* and *Nitzshia* (diatoms), and *Thraustochytriaceae* (Cercozoa), as well as the cnidarian genus *Bougainvillia*. Bacteria were mostly members of the family *Saprospiraceae* and especially several ASV of the genus *Lewinella*. Some genera of Rhabditophanes (e.g. *Chromadorea)* were positively correlated with microeukaryotes and bacteria.

Discussion

Biofouling biomass and EPS production are not linearly controlled by shear stress intensity

In the literature, studies on biofouling formed in natural environments have mainly focused on the influence of environmental parameters on biofilm biomass, rather than on properties specifically associated with hydrodynamic forces such as shear stress, turbulence or mixing intensity. Consequently, the hydrodynamic aspects, particularly those in situ in marine environments, remain largely understudied and poorly characterised. This contributes to a lack of detailed information that presents challenges when comparing findings across various experiments. While previous studies in freshwater ecosystems have demonstrated a decrease in bacterial and microalgal biomass with increasing flow velocities [33, 34], studies in drinking water systems have shown the opposite effect on bacterial biomass [35]. These disparities can be attributed to variations in the hydrodynamic regime associated with flow velocity, for example, or to differences in the composition of microbial communities and the complex interactions between different species in biofilms. In our case, attached biomass showed a seasonal pattern, with higher values during summer compared to winter/autumn, suggesting that growth of biofilms and associated multicellular organisms have been promoted by temperature and increased of seawater primary productivity irrespective of hydrodynamics [36]. Interestingly, our study revealed a two-step response at each season, with an increase in biomass when transitioning from static to lowest shear stress conditions, and a decrease in biomass when shear stress intensity increased. The increase in biomass may probably be due to better availability of nutrients and oxygen, which promotes biofilm development [13, 14]. Additionally, a higher predation pressure due to vagile species may

limit the biomass in static condition. These mobile taxa could exploit the protective environment provided by biofilms for feeding [37]. As the occurrence of these predators was limited in dynamic conditions, microbial growth could be favored. The increase of shear stress intensity (S_2 to S_4) induced a biomass decrease because the adhesion of new organisms may be limited together with an increase of cells detachment [10, 38]. This decrease in biofilm thickness was positively correlated with an overproduction of EPS, primarily exopolysaccharides [11, 39]. This adaptive response, characterized by an increase in EPS production in response to rising shear forces, may allow biofilms to withstand shear forces and minimize detachment from the colonized surface, as it has been already observed in *Pseudomonas fluorescens* biofilms exposed to different linear flow velocities [40]. These changes in EPS matrix composition appear to be associated with changes in the dominance of microbial groups, particularly diatoms and bacteria, which then may modify their EPS production depending on shear stress. This is consistent with a recent study on microphytobenthic biofilms, which reported different EPS production dynamics by bacteria and diatoms depending on the type of intertidal sediment [41]. According to these authors, the differences are related to changes in community functioning, and particularly to the use of EPS either for mobility or substrate attachment. However, their findings are based on changes in the relative composition of microbial fatty acids in different EPS fractions, unfortunately without link to microbial taxa.

Furthermore, we observed significant differences between EPS samples based on their immersion mode, mainly qualitative in the exopolymers produced. Under dynamic conditions, both colloidal and loosely bound EPS fractions showed higher protein contents in spring and summer, whereas under static conditions, higher carbohydrate contents, especially uronic acids, were observed throughout the year. Uronic acids, when binding with divalent cations, form bridges that improve interactions between EPS components, thereby increasing the mechanical stability of biofilms [42]. These molecules, which are found in free form in the water column [43], could be captured more efficiently under static conditions. Their detection within the EPS fractions could therefore suggest that they were integrated into the matrix polysaccharides. However, while uronic acids are important for the internal cohesion of the EPS matrix, they do not provide overall mechanical cohesion under shear stress, as demonstrated in a previous study [28]. Other cohesive components and mechanisms may also play a synergistic role in the formation of an adhesive and cohesive EPS matrix of biofilms.

Community structure is influenced as much by immersion mode as physico-chemical parameters, but less by shear stress intensity

While richness was not significantly affected, prokaryotic diversity decreased notably at higher shear stresses compared to static conditions, likely due to enhanced microbial cell detachment, as previously reported but with higher shear forces (15 knots, i.e. 8 m s^{-1}) not representative of mediterranean hydrodynamics [20]. However, during extreme storm events, high shear stress may drastically reduce the diversity of biofouling communities, as has been observed in macrobenthic assemblages [44].

At each season, we observed a notable divergence in community structure between static and dynamic modes, highlighting the role of the transition between the two conditions, more than the magnitude of the shear stress intensity. A large core community was present, but a significant number of specific taxa was also observed under dynamic mode regardless of season: more than a quarter of reads for prokaryotes and about a fifth for eukaryotes. However, specific ASVs or reads at different shear stress intensities were remarkably low, highlighting the transition from static to dynamic conditions as a more critical selection factor than shear stress intensity. Our results also demonstrated that shear stress induced a selection on microbial communities as significant as classical physico-chemical seawater parameters like temperature, salinity or nutrients, which were reported to date as the main drivers for biofilm communities [19, 45]. Moreover, the term "static" must be used with care, as currents and turbulence could occur at the immersion site. However, the Toulon Bay is protected from the currents by a dike. Therefore, the hydrodynamic conditions are less pronounced than at an offshore site, where the absence of such protection could lead to greater water movement and turbulence.

Adhesion was not the only function to be selected by shear stress

A relatively high proportion of taxa was specific to dynamic conditions (38–54%). We hypothesized that high shear stress has selected taxa with the capacity to resist to physical pull-out, due to the presence of external anchoring structure (pili or curli) or the ability to produce EPS [46], both in order to have strong surface adhesion and aggregation. These abilities correspond to those of early biofilm bacteria and may be shared by some *Rhodobacteriaceae*, including *Salinihabitans*, *Roseovarius*, and *Litoreibacter*, which were found to dominate stressed biofilm communities in this and previous studies [20, 47]. Interestingly, *Pseudoalteromonas* typically recognized as initial colonizers of artificial surfaces, were discriminant taxa in dynamic samples [48]. Nevertheless, no member

of the *Alteromonadaceae*, considered as primary pioneers of marine biofilms, were observed in our samples [48, 49]. Filamentous bacteria like *Leucothrix* and *Thiotrix* [50], found exclusively in dynamic samples, have already been described as ectosymbionts associated with the cuticle of nematodes [51] but also with the surface of brown algae [52], justifying their strong colonizing capacity. These observations suggested that shear stress induced a complex biofilm maturation process, favoring some pioneer taxa but also probably taxa with specific adhesion capacities to resist shear stress. Further studies are needed to also determine the temporal dynamics of colonization under shear stress.

The dynamic stress clearly influence biofilm development through a restricted recruitment and settlement of larvae and propagules [53]. This phenomenon probably explained the increased abundance of brown and red algae in static samples. For example, the abundance of *Leathesia* and *Pylaiella* (Phaeophyceae) was higher in the static samples and corresponded to the specific occurrence of a lyso-DGTA, a chemical family commonly found in brown algal communities [54]. Specific taxa under shear stress showed distinctive morphological adaptations (e.g., by muscular contraction, deformation, and/or rapid growth). Notably, solitary soft-bodied species (*e.g., Ceramium* (Florideophyceae)), and mobile species (*e.g.,* the nematode *Chromadorina* and the gastropod *Eubranchus*) were abundant and characteristic in static samples. Conversely, colonial species, such as ascidians, hydrozoans, and bryozoans, which are encrusting and flexible species, were abundant in dynamic samples. Phenotypic plasticity is also an important strategy to resist to rapid environmental changes, illustrated by the morphological plasticity of colonial hydrozoans in dynamic environments [55]. Moreover, benthic diatoms exhibited enhanced adhesion mechanisms, potentially due to the EPS they produce, leading to a significantly improved adhesion of the genera *Navicula* and *Tabularia* under dynamic stress. This finding was consistent with previous studies showing that marine biofilms grown under dynamic conditions exhibited increased adhesion forces and diatom abundances compared to static conditions [56, 57]. Additionally, the detection of DMSP in dynamic samples could confirm the presence of this group, which can be released in response to physiological and mechanical stress, leading to increased production of DMSP [58].

Despite the use of a rinsing step in our protocol to remove vagile organisms, we observed a substantial presence of arthropod-associated genera, including copepods and amphipods detected through 18S rRNA and COI genes mainly in static samples. In contrast, dynamic samples showed an increased abundance of small vagile or planktonic organisms, including ciliates, dinophyceans, and amoebae. Heterotrophic protists, such as ciliates, flagellates, and amoebae, use long ventral cilia for adhesion, facilitating attachment under high shear stress conditions [59]. Some of these protists are endosymbionts (*e.g. Sacocystis* and *Hypocoma*) that may infect dinoflagellates, ciliates, and marine copepods [60]. Our hypothesis is that the gregarious and complex establishment of sessile invertebrates and macroalgae in biofouling communities provides structural habitat and protection for mobile taxa but also provides other benefits, including high food concentrations that can be several orders of magnitude higher than those found in the surrounding water [61]. However, these mobile organisms are known to move in and out of the biofilm, making it difficult to precisely determine their actual role in predation processes within the biofilm. While their presence suggests active predation, the transient nature of their interactions complicates the analysis of their impact on biofilm composition and dynamics. Furthermore, cells may also become captive within the matrix through brownian-type interactions, which are most effective at low flow velocities [10]. Thus, biofilm and biofouling processes involve complex interactions within the biofilm matrix of vagile and planktonic organisms. These dynamics can be induced by deterministic processes associated with imposed shear stress, but they can also result from random contact in seawater due to stochastic factors.

Dynamic conditions enhance the recruitment of harmful microorganisms and non-indigenous species

Our study revealed that dinoflagellates were highly abundant in biofilms in spring, especially in dynamic samples. The *Biecheleria* genus was remarkable for its absence in the Toulon Bay planktonic environment but dominance in our biofilms [62]. This suggests that this genus was selectively advantaged and adapted to the biofilm lifestyle, similar to some bacteria and eukaryotes identified in this area [63]. However, genera commonly found in planktonic blooms, such as *Alexandrium* and *Prorocentrum*, are also present in Toulon Bay. A high abundance was also observed for the genus *Vibrio*, which includes some pathogenic species associated with mortality of farmed species (e.g. mussels, oysters, or fish) such as *V.owensii*, *V.crassostreae*, and *V.campbellii* species enriched in our dynamic samples. The presence of these genera in biofilms can be attributed to adsorption in the matrix, which correlates with their higher abundance in the environment. Furthermore, biofilms are highly effective at trapping environmental DNA and preventing its degradation [64]. This enables the potential detection of both bloom-forming species and perhaps rare species that might otherwise remain undetected. Low intensity of phytoplankton proliferation limits this risk in Toulon Bay.

Changes in the nature of EPS during high shear stress made it thicker and more cohesive, which could promote particles adsorption and entrapment of organisms within biofilms. Thus, marine fouling poses potential risks to human health and farmed species as a vector for harmful organisms [65]. However, our analysis of metabolites did not detect any toxins, particularly saxitoxin. The assessment of potential risks could be conducted by measuring toxin production specifically.

Additionally, the present study showed that some non-indigenous species (NIS), already reported in harbours in the Mediterranean Sea, thrived under shear stress. *Watersipora subtorquata* and *Bugula neritinia* were specifically better represented in dynamic conditions in autumn and winter. NIS are known for their adaptability, resilience, and ability to outcompete native species [66]. Their adaptation to shear conditions is probably due to their ecological traits, which enable them to colonize vessel hulls and offshore structures, as it has already been recorded in North Sea offshore wind farms [67, 68].

Shear stress limits predation and chemical defense

The use of multi-block analyses and the building of correlation network, selecting the most discriminating metabolites and ASVs, confirmed that community dynamics were strongly shaped by the immersion mode. Some specific metabolites were identified in the cluster characteristic of static conditions, *e.g.,* pheophorbide a, which is considered as the main product formed after chlorophyll a degradation to pheophytin a. This pigment is indeed often found in the fecal pellets of copepods or nematodes of the genus *Chromadorina*, as a result of the degradation of chlorophyll in their stomach [69, 70]. The high expression of this compound was then in agreement with the results obtained by metabarcoding which showed a higher proportion of these taxa in static samples than in dynamic ones. It is important to note that, in static condition, additional factors such as enhanced predation or grazing by fish larvae and macro-invertebrates, as well as the sorption of organic particles on the surfaces, probably contributed to the observed differences in biofilm composition. Other genera, such as *Ochrovirga*, *Winogradskyella*, or *Granulosicoccus*, positively correlated with several brown algae (i.e., *Leathesia* and *Heribaudiella*) and pheophorbide a, and have been reported to colonize algal surfaces in several studies [54, 71, 72]. Thus, the presence of pheophorbide a in these samples may result from microbial degradation on the algal surface and grazing by invertebrates and nematodes. We also observed a positive correlation between the presence of some metabolites, like Stigmatellin Y, and both bacteria and a specific associated with a brown alga of the *Acinetosporaceae* family. Stigmatellins are compounds generated by bacteria and are known for their potential antibiofilm actions [73]. This correlation suggests that bacteria associated with the algae surface may enhance the chemical defenses of the algae against fouling by producing metabolites that have ecological activity [74].

Grazing by heterotrophic protists shapes the abundance and structure of microbial communities, and the increase in shear force led to an increase in the abundance of ciliates. Some of these vagile taxa were positively correlated with several bacteria, including *Saprospiraceae* in the dynamic conditions cluster. *Sapropiraceae* dominate microbial communities on PVC surfaces and contribute to EPS production in biofilm [75, 76]. It is possible that an increased stress limits chemosensory mechanisms for identifying prey, which involves selection of bacteria trapped in the matrix [77]. Heterotrophic protozoa are, therefore, thought to actively select bacteria and are able to move through the matrix [78]. The specific mechanism of ciliate bacterial selection remains unknown, but a previous work has suggested they primarily feed on EPS rather than on planktonic cells in biofilms under continuous flow [79]. This finding suggests that an increased shear stress alters nutrient availability, affecting the diet of heterotrophic protists. Bacteria may benefit from reduced grazing under shear stress by developing resistant structures through overproduction of EPS.

Conclusion

Our work provided new insight into marine biofilm ecology, highlighting the significant role of shear stress in shaping natural biofilm communities. The multi-omics approach demonstrated that the transition from static to dynamic conditions has a higher impact on community diversity than changes in shear stress intensity or seasonal physico-chemical parameters. Dynamic conditions resulted in thinner, protein-rich biofilms primarily composed of taxa with strong adhesion mechanisms, like bacteria and diatoms. Conversely, static conditions enhanced the presence of vagile microeukaryotes and macroorganisms. Metabolic expression indirectly revealed that shear stress can limit predation and influence chemical defense mechanisms within biofilms. Furthermore, we observed an enrichment of harmful species and non-indigenous microorganisms under shear stress, emphasizing potential ecological and health risks. These findings underscore the complex interplay between hydrodynamics, microbial communities, and macroorganisms in marine biofilms, highlighting the need for a deeper understanding to the colonization dynamics of biofouling communities in marine ecosystems.

Supplementary Information

The online version contains supplementary material available at https://doi.org/10.1186/s40793-024-00647-5.

Additional file 1.

Additional file 2.

Additional file 3.

Additional file 4.

Additional file 5.

Acknowledgements
The authors thank Dr S. Greff (Aix-Marseille University, IMBE, France) for the LC-MS experiments which were conducted on the regional metabolomics platform MALLABAR [Funds: Institute of Ecology and Environment (INEE) of the French National Centre for Scientific Research (CNRS), Total Foundation and the French Sud-PACA regional council].

Author contributions
AP, GC, NQ, JF conceived and designed the study. AP conducted the experiments, data collection, statistical analysis and data visualization, wrote the original manuscript, edited and reviewed the manuscript. GC, NQ, JF, AOM edited and reviewed the manuscript. NC performed metabolomic analysis. H.H and RBM performed confocal laser scanning microscopy analysis. DB performed low vacuum scanning electron microscopy analysis.

Funding
This work benefited from France Energies Marines and State financing managed by the National Research Agency under the Investments for the Future program bearing the reference ANR-10-IED-0006–32. This work was carried out in the frame of the ABIOP + project.

Availability of data and materials
The datasets generated during the current study are available in the SRA (BioProject PRJNA1052431) using the MIxS package.

Declarations

Ethics approval and consent to participate
Not applicable.

Consent for publication
Not applicable.

Competing interests
The authors declare that they have no competing interests.

Author details
[1]France Energies Marines, Plouzané, France. [2]Laboratoire MAPIEM, Université de Toulon, Toulon, France. [3]Université de Toulon, Aix Marseille Univ., CNRS, IRD, MIO, Toulon, France. [4]Laboratoire d'Analyses de Surveillance et d'Expertise de La Marine (LASEM), Toulon, France. [5]IMBE, Aix Marseille Université, Avignon Université, CNRS, IRD, Avignon, France.

Received: 9 July 2024 Accepted: 21 November 2024
Published online: 18 December 2024

References

1. Flemming H-C, van Hullebusch ED, Little BJ, Neu TR, Nielsen PH, Seviour T, Stoodley P, Wingender J, Wuertz S. Microbial extracellular polymeric substances in the environment, technology and medicine. Nat Rev Microbiol. 2024. https://doi.org/10.1038/s41579-024-01098-y.
2. Gerbersdorf SU, Koca K, de Beer D, Chennu A, Noss C, Risse-Buhl U, et al. Exploring flow-biofilm-sediment interactions: assessment of current status and future challenges. Water Res. 2020;185:116182.
3. Zhang W, Ding W, Li YX, Tam C, Bougouffa S, Wang R, et al. Marine biofilms constitute a bank of hidden microbial diversity and functional potential. Nat Commun. 2019;10(1):517.
4. Caruso G. Microbial colonization in marine environments: Overview of current knowledge and emerging research topics. J Mar Sci Eng. 2020;8(2):78.
5. Noack M, Gerbersdorf SU, Hillebrand G, Wieprecht S. Combining field and laboratory measurements to determine the erosion risk of cohesive sediments best. Water. 2015;7(9):5061–77.
6. He C, Taylor JN, Rochfort Q, Nguyen D. A new portable *in situ* flume for measuring critical shear stress on river beds. Int J Sediment Res. 2021;36(2):235–42.
7. Tolhurst TJ, Black KS, Paterson DM, Mitchener HJ, Termaat GR, Shayler SA. A comparison and measurement standardisation of four in situ devices for determining the erosion shear stress of intertidal sediments. Cont Shelf Res. 2000;20(10):1397–418.
8. Chun ALM, Mosayyebi A, Butt A, Carugo D, Salta M. Early biofilm and streamer formation is mediated by wall shear stress and surface wettability: a multifactorial microfluidic study. MicrobiologyOpen. 2022;11(4):e1310.
9. Simões LC, Gomes IB, Sousa H, Borges A, Simões M. Biofilm formation under high shear stress increases resilience to chemical and mechanical challenges. Biofouling. 2022;38(1):1–12.
10. Krsmanovic M, Biswas D, Ali H, Kumar A, Ghosh R, Dickerson AK. Hydrodynamics and surface properties influence biofilm proliferation. Adv Colloid Interface Sci. 2021;288:102336.
11. Liu Y, Tay JH. The essential role of hydrodynamic shear force in the formation of biofilm and granular sludge. Water Res. 2002;36(7):1653–65.
12. Fang H, Chen Y, Huang L, He G. Analysis of biofilm bacterial communities under different shear stresses using size-fractionated sediment. Sci Rep. 2017;7(1):1299.
13. Tsagkari E, Connelly S, Liu Z, McBride A, Sloan WT. The role of shear dynamics in biofilm formation. NPJ Biofilms Microbiomes. 2022;8(1):1–10.
14. Stoodley P, Dodds I, Boyle JD, Lappin-Scott HM. Influence of hydrodynamics and nutrients on biofilm structure. J Appl Microbiol. 1998;85(S1):19S-28S. https://doi.org/10.1111/j.1365-2672.1998.tb05279.x.
15. Simões M, Pereira MO, Sillankorva S, Azeredo J, Vieira MJ. The effect of hydrodynamic conditions on the phenotype of *Pseudomonas fluorescens* biofilms. Biofouling. 2007;23(4):249–58.
16. Lecuyer S, Rusconi R, Shen Y, Forsyth A, Vlamakis H, Kolter R, et al. Shear stress increases the residence time of adhesion of *Pseudomonas aeruginosa*. Biophys J. 2011;100(2):341–50.
17. Hearin J, Hunsucker KZ, Swain G, Gardner H, Stephens A, Lieberman K. Analysis of mechanical grooming at various frequencies on a large scale test panel coated with a fouling-release coating. Biofouling. 2016;32(5):561–9.
18. Shields MA, Woolf DK, Grist EPM, Kerr SA, Jackson AC, Harris RE, et al. Marine renewable energy: the ecological implications of altering the hydrodynamics of the marine environment. Ocean Coast Manag. 2011;54(1):2–9.
19. Zhang B, Yang X, Liu L, Chen L, Teng J, Zhu X, et al. Spatial and seasonal variations in biofilm formation on microplastics in coastal waters. Sci Total Environ. 2021;770:145303.
20. Catão ECP, Pollet T, Misson B, Garnier C, Ghiglione J-F, Barry-Martinet R, Maintenay M, Bressy C, Briand J-F. Shear stress as a major driver of marine biofilm communities in the NW Mediterranean Sea. Front Microbiol. 2019. https://doi.org/10.3389/fmicb.2019.01768.
21. Hunsucker JT, Hunsucker KZ, Gardner H, Swain G. Influence of hydrodynamic stress on the frictional drag of biofouling communities. Biofouling. 2016;32(10):1209–21.
22. Naik AT, Kamensky KM, Hellum AM, Moisander PH. Disturbance frequency directs microbial community succession in marine biofilms exposed to shear. mSphere. 2023;8(6):e00248-e323. https://doi.org/10.1128/msphere.00248-23.
23. Clementi E, Goglio AC, Aydogdu A, Pistoia J, Escudier R, Drudi M, et al. The new Mediterranean Sea analysis and forecasting system including tides: description and validation. Copernicus Meetings; 2021. Report No.: EGU21–13531.
24. Korres G, Ravdas M, Zacharioudaki A. Mediterranean Sea waves analysis and forecast (CMEMS MED-Waves). Copernicus Monitoring Environment Marine Service (CMEMS); 2019.

25. Parada AE, Needham DM, Fuhrman JA. Every base matters: assessing small subunit rRNA primers for marine microbiomes with mock communities, time series and global field samples. Environ Microbiol. 2016;18(5):1403–14.
26. Van de Peer Y, De Rijk P, Wuyts J, Winkelmans T, De Wachter R. The European small subunit ribosomal RNA database. Nucleic Acids Res. 2000;28(1):175–6.
27. Leray M, Yang JY, Meyer CP, Mills SC, Agudelo N, Ranwez V, et al. A new versatile primer set targeting a short fragment of the mitochondrial COI region for metabarcoding metazoan diversity: application for characterizing coral reef fish gut contents. Front Zool. 2013;10(1):34.
28. Portas A, Carriot N, Ortalo-Magné A, Damblans G, Thiébaut M, Culioli G, et al. Impact of hydrodynamics on community structure and metabolic production of marine biofouling formed in a highly energetic estuary. Mar Environ Res. 2023;192:106241.
29. Pluskal T, Castillo S, Villar-Briones A, Orešič M. MZmine 2: Modular framework for processing, visualizing, and analyzing mass spectrometry-based molecular profile data. BMC Bioinf. 2010;11(1):395.
30. Carriot N, Barry-Martinet R, Briand JF, Ortalo-Magné A, Culioli G. Impact of phosphate concentration on the metabolome of biofilms of the marine bacterium *Pseudoalteromonas lipolytica*. Metabolomics. 2022;18(3):18.
31. Chong J, Soufan O, Li C, Caraus L, Li S, Bourque G, Wishart DS, Xia J. MetaboAnalyst 4.0: towards more transparent and integrative metabolomics analysis. Nucleic Acids Res. 2018;46(W1):W486–94. https://doi.org/10.1093/nar/gky310.
32. Singh A, Shannon CP, Gautier B, Rohart F, Vacher M, Tebbutt SJ, et al. DIABLO: an integrative approach for identifying key molecular drivers from multi-omics assays. Bioinformatics. 2019;35(17):3055–62.
33. Battin TJ, Kaplan LA, Newbold JD, Cheng X, Hansen C. Effects of current velocity on the nascent architecture of stream microbial biofilms. Appl Environ Microbiol. 2003;69(9):5443–52.
34. Besemer K, Singer G, Hödl I, Battin TJ. Bacterial community composition of stream biofilms in spatially variable-flow environments. Appl Environ Microbiol. 2009;75(22):7189–95.
35. Fish K, Osborn AM, Boxall JB. Biofilm structures (EPS and bacterial communities) in drinking water distribution systems are conditioned by hydraulics and influence discolouration. Sci Total Environ. 2017;593–594:571–80.
36. Gerbersdorf SU, Wieprecht S. Biostabilization of cohesive sediments: revisiting the role of abiotic conditions, physiology and diversity of microbes, polymeric secretion, and biofilm architecture. Geobiology. 2015;13(1):68–97.
37. Smee DL, Ferner MC, Weissburg MJ. Hydrodynamic sensory stressors produce nonlinear predation patterns. Ecology. 2010;91(5):1391–400.
38. Thomen P, Robert J, Monmeyran A, Bitbol AF, Douarche C, Henry N. Bacterial biofilm under flow: first a physical struggle to stay, then a matter of breathing. PLoS ONE. 2017;12(4):e0175197.
39. Ramasamy P, Zhang X. Effects of shear stress on the secretion of extracellular polymeric substances in biofilms. Water Sci Technol. 2005;52(7):217–23.
40. Araújo PA, Malheiro J, Machado I, Mergulhão F, Melo L, Simões M. Influence of flow velocity on the characteristics of *Pseudomonas fluorescens* biofilms. J Environ Eng. 2016;142(7):04016031.
41. Hubas C, Gaubert-Boussarie J, D'Hondt AS, Jesus B, Lamy D, Meleder V, et al. Identification of microbial exopolymer producers in sandy and muddy intertidal sediments by compound-specific isotope analysis. dobret. 2022;2022.12.02.516908.
42. Flemming H-C, Neu TR, Wingender J. The perfect slime: Microbial extracellular polymeric substances (EPS). Water Intell Online. 2016;15(0):9781780407425. https://doi.org/10.2166/9781780407425.
43. Hung CC, Tang D, Warnken KW, Santschi PH. Distributions of carbohydrates, including uronic acids, in estuarine waters of Galveston Bay. Mar Chem. 2001;73(3):305–18.
44. Corte GN, Schlacher TA, Checon HH, Barboza CAM, Siegle E, Coleman RA, et al. Storm effects on intertidal invertebrates: increased beta diversity of few individuals and species. PeerJ. 2017;5:e3360.
45. Lawes JC, Neilan BA, Brown MV, Clark GF, Johnston EL. Elevated nutrients change bacterial community composition and connectivity: high throughput sequencing of young marine biofilms. Biofouling. 2016;32(1):57–69.
46. Conrad JC. Physics of bacterial near-surface motility using flagella and type IV pili: implications for biofilm formation. Res Microbiol. 2012;163(9):619–29.
47. Doghri I, Rodrigues S, Bazire A, Dufour A, Akbar D, Sopena V, et al. Marine bacteria from the French Atlantic coast displaying high forming-biofilm abilities and different biofilm 3D architectures. BMC Microbiol. 2015;15(1):231.
48. Pollet T, Berdjeb L, Garnier C, Durrieu G, Le Poupon C, Misson B, Briand J-F. Prokaryotic community successions and interactions in marine biofilms: the key role of *Flavobacteriia*. FEMS Microbiol Ecol. 2018. https://doi.org/10.1093/femsec/fiy083.
49. Briand J-F, Pollet T, Misson B, Garnier C, Lejars M, Maintenay M, Barry-Martinet R, Portas A, Ghiglione J-F, Bressy C. Surface characteristics together with environmental conditions shape marine biofilm dynamics in coastal NW Mediterranean locations. Front Mar Sci. 2022. https://doi.org/10.3389/fmars.2021.746383.
50. Watsuji TO, Motoki K, Hada E, Nagai Y, Takaki Y, Yamamoto A, et al. Compositional and functional shifts in the epibiotic bacterial community of *Shinkaia crosnieri* Baba & Williams (a squat lobster from hydrothermal vents) during methane-fed rearing. Microbes Environ. 2018;33(4):348–56.
51. Bellec L, Bonavita MAC, Hourdez S, Jebbar M, Tasiemski A, Durand L, et al. Chemosynthetic ectosymbionts associated with a shallow-water marine nematode. Sci Rep. 2019;9(1):7019.
52. Paix B, Layglon N, Le Poupon C, D'Onofrio S, Misson B, Garnier C, et al. Integration of spatio-temporal variations of surface metabolomes and epibacterial communities highlights the importance of copper stress as a major factor shaping host-microbiota interactions within a Mediterranean seaweed holobiont. Microbiome. 2021;9(1):201.
53. Wheeler JD, Secchi E, Rusconi R, Stocker R. Not just going with the flow: the effects of fluid flow on bacteria and plankton. Annu Rev Cell Dev Biol. 2019;35(1):213–37.
54. Paix B, Carriot N, Barry-Martinet R, Greff S, Misson B, Briand J-F, Culioli G. A multi-omics analysis suggests links between the differentiated surface metabolome and epiphytic microbiota along the thallus of a Mediterranean seaweed holobiont. Front Microbiol. 2020. https://doi.org/10.3389/fmicb.2020.00494.
55. Eder Y, Tschink D, Gerlach G, Strahl J. Physiology of juvenile hydroids—high food availability mitigates stress responses of *Hydractinia echinata* to increasing seawater temperatures. J Exp Mar Biol Ecol. 2018;508:64–72.
56. Zargiel KA, Swain GW. Static vs dynamic settlement and adhesion of diatoms to ship hull coatings. Biofouling. 2014;30(1):115–29.
57. Hunsucker KZ, Koka A, Lund G, Swain G. Diatom community structure on in-service cruise ship hulls. Biofouling. 2014;30(9):1133–40.
58. Stefels J. Physiological aspects of the production and conversion of DMSP in marine algae and higher plants. J Sea Res. 2000;43(3):183–97.
59. Risse-Buhl U, Scherwass A, Schlüssel A, Arndt H, Kröwer S, Küsel K. Detachment and motility of surface-associated ciliates at increased flow velocities. Aquat Microb Ecol. 2009;55:209–18.
60. Clarke LJ, Bestley S, Bissett A, Deagle BE. A globally distributed *Syndiniales* parasite dominates the Southern Ocean micro-eukaryote community near the sea-ice edge. ISME J. 2019;13(3):734–7.
61. Loke LHL, Todd PA. Structural complexity and component type increase intertidal biodiversity independently of area. Ecology. 2016;97(2):383–93.
62. Serranito B, Jamet JL, Rossi N, Jamet D. Decadal shifts of coastal microphytoplankton communities in a semi-enclosed bay of NW Mediterranean Sea subjected to multiple stresses. Estuar Coast Shelf Sci. 2019;224:171–86.
63. Briand JF, Pochon X, Wood SA, Bressy C, Garnier C, Réhel K, et al. Metabarcoding and metabolomics offer complementarity in deciphering marine eukaryotic biofouling community shifts. Biofouling. 2018;34(6):657–72.
64. Rivera SF, Rimet F, Vasselon V, Vautier M, Domaizon I, Bouchez A. Fish eDNA metabarcoding from aquatic biofilm samples: Methodological aspects. Mol Ecol Resour. 2022;22(4):1440–53.
65. Naik RK, Naik MM, D'Costa PM, Shaikh F. Microplastics in ballast water as an emerging source and vector for harmful chemicals, antibiotics, metals, bacterial pathogens and HAB species: a potential risk to the marine environment and human health. Mar Pollut Bull. 2019;149:110525.
66. Leclerc JC, Viard F, González Sepúlveda E, Díaz C, Neira Hinojosa J, Pérez Araneda K, et al. Habitat type drives the distribution of non-indigenous species in fouling communities regardless of associated maritime traffic. Divers Distrib. 2020;26(1):62–75.

67. De Mesel I, Kerckhof F, Norro A, Rumes B, Degraer S. Succession and seasonal dynamics of the epifauna community on offshore wind farm foundations and their role as stepping stones for non-indigenous species. Hydrobiologia. 2015;756(1):37–50.
68. Vinagre PA, Simas T, Cruz E, Pinori E, Svenson J. Marine biofouling: a European database for the marine renewable energy sector. J Mar Sci Eng. 2020;8(7):495.
69. Gieskes WWC, Engelkes MM, Grakaay GW. Degradation of diatom chlorophyll to colourless, non-fluorescing compounds during copepoo grazing. Hydrobiol Bull. 1991;25(1):65–72.
70. Majdi N, Tackx M, Traunspurger W, Buffan-Dubau E. Feeding of biofilm-dwelling nematodes examined using HPLC-analysis of gut pigment contents. Hydrobiologia. 2012;680(1):219–32.
71. Kwon Y-K, Kim JH, Kim JJ, Yang S-H, Ye B-R, Heo S-J, Hyun J-H, Qian Z-J, Park H-S, Kang D-H, Chulhong O. *Ochrovirga pacifica* gen. nov., sp. nov., a novel agar-lytic marine bacterium of the family *Flavobacteriaceae* isolated from a seaweed. Curr Microbiol. 2014;69(4):445–50. https://doi.org/10.1007/s00284-014-0598-4.
72. Park S, Jung Y-T, Won S-M, Park J-M, Yoon J-H. *Granulosicoccus undariae* sp. nov., a member of the family *Granulosicoccaceae* isolated from a brown algae reservoir and emended description of the genus *Granulosicoccus*. Antonie Leeuwenhoek. 2014;106(5):845–52. https://doi.org/10.1007/s10482-014-0254-9.
73. Boopathi S, Vashisth R, Manoharan P, Kandasamy R, Sivakumar N, Stigmatellin Y. An anti-biofilm compound from *Bacillus subtilis* BR4 possibly interferes in PQS–PqsR mediated quorum sensing system in Pseudomonas aeruginosa. Bioorg Med Chem Lett. 2017;27(10):2113–8.
74. Kumar V, Rao D, Thomas T, Kjelleberg S, Egan S. Antidiatom and antibacterial activity of epiphytic bacteria isolated from *Ulvalactuca* in tropical waters. World J Microbiol Biotechnol. 2011;27(7):1543–9.
75. Qian P-Y, Cheng A, Wang R, Zhang R. Marine biofilms: diversity, interactions and biofouling. Nat Rev Microbiol. 2022;20(11):671–84. https://doi.org/10.1038/s41579-022-00744-7.
76. Zhu X, Lee LW, Song G, Zhang X, Gao Y, Yang G, et al. Deciphering mono/multivalent draw solute-induced microbial ecology and membrane fouling in anaerobic osmotic membrane bioreactor. Water Res. 2022;209:117869.
77. Dopheide A, Lear G, Stott R, Lewis G. Preferential feeding by the ciliates *Chilodonella* and *Tetrahymena* spp. and effects of these protozoa on bacterial biofilm structure and composition. Appl Environ Microbiol. 2011;77(13):4564–72. https://doi.org/10.1128/AEM.02421-10.
78. Huws SA, McBain AJ, Gilbert P. Protozoan grazing and its impact upon population dynamics in biofilm communities. J Appl Microbiol. 2005;98(1):238–44. https://doi.org/10.1111/j.1365-2672.2004.02449.x.
79. Joubert LM, Wolfaardt GM, Botha A. Microbial exopolymers link predator and prey in a model yeast biofilm system. Microb Ecol. 2006;52(2):187–97.

Publisher's Note